Fan blade damage detection using on-line vibration monitoring

W.G. Smit[1] P.S. Heyns[1]

(First received November 2001; Final version September 2002)

The use of on-line vibration monitoring of fan blades to detect and classify damage levels on blades was investigated. It was shown that output only data can be used to determine modal parameters, such as natural frequencies, with sufficient accuracy to be used as damage indicators. This is only possible if sensors are mounted on the blades themselves, thereby ensuring that the dynamics of the blades can be accurately monitored. A finite element model was used to study the feasibility of using frequency shifts as damage indicators on rotating fan blades. The results indicated that certain mode shapes are more sensitive to damage at the root of the blade. An experimental fan blade damage simulator was then used to verify these findings experimentally. A hypothesis, that the differences in frequency shift due to damage between the finite element model and the experimentally measured frequencies is the result of global structural behaviour, was verified by making use of an extended finite element model. Local mode shapes make it possible to classify damage levels on individual blades using one sensor per blade only. Damage levels of as low as 10% could be detected experimentally.

Nomenclature

A	AR coefficient matrix
$a_1, a_2..., a_n$	AR coefficients
B	MA coefficient matrix
$b_1, b_2..., b_n$	MA coefficients
C	ARMA coefficient matrix
$c_1, c_2..., c_n$	ARMA coefficients
$e(t)$	Sequence of white noise
n	Number of coefficients in AR, MA, ARMA model
na	Number of AR coefficients
nb	Number of MA coefficients
nc	Number of ARMA coefficients
p	Order of AR model
q	Order of MA model
s	Variance
t	Time index
t_n	Normal distribution curve
$x(k)$	Random variables
$x(t)$	Function values
$\bar{x}$	Mean of $x(k)$

Greek symbols

α	Empirically calculated value for normal distribution curves
θ	Parameter vector
σ_x	Standard deviation of x
μ_x	Average value of x

1. Dynamic Systems Group, Department of Mechanical and Aeronautical Engineering, University of Pretoria, Pretoria, 0002 South Africa

Introduction

Continuous monitoring of the condition of critical equipment is becoming increasingly important in industry. Failure of such equipment may have dire consequences for the whole process. The Forced and Induced Draught fans used on power station boilers are examples of such critical equipment.

Vibration measurement is often utilised to identify the presence of bearing faults on such equipment. Conventional vibration measurement approaches are however not suitable for the identification of localised damage on the fan blades. This is traditionally the domain of non-destructive damage detection methods such as ultrasonic scanning, x-ray diffraction, or dye penetrant inspection methods. These techniques cannot however be implemented on operating fan blades. Defects may further be overlooked owing to shielding by the structure itself or inexperience of the operator.

This gives rise to the question whether vibration monitoring can be used for the detection of fan blade damage on operating fans. Vibration monitoring of structures and machines has received considerable attention in the last few decades. Doebling *et al.*[1] have presented an extensive survey of this field. The ability of these methods to do global monitoring of a structure using relatively few sensors at fixed measurement positions during normal operation of the machine, as opposed to methods (such as x-ray inspection) that require scanning of the entire structure under stationary conditions, is a huge advantage.

It is usually difficult to find a vibration-related characteristic that changes significantly with increasing levels of damage. Friswell & Penny[2] reviewed the state of the art in damage detection and location using vibration data. They noted that algorithms should be tailored to a specific application, as it is unlikely that a single best method for all applications will ever emerge.

Many investigators have considered the use of changes in natural frequency as damage indicator. The observation that changes in structural properties cause changes in natural frequencies was indeed the stimulus for using modal methods for damage identification and health monitoring.

However, researchers soon found that frequency changes have significant practical limitations for structures such as bridges, offshore oil platforms and other large civil engineering structures. The low sensitivity of frequency shifts to damage required either very precise measurements or high levels of damage.

e Silva & Gomes[3] however found that the level of damage on a simple cantilever beam could be determined accurately using shifts in natural frequencies. If more than one frequency was used the location could also be determined. This suggests the possibility of using blade vibration frequency measurements to identify the presence of damage on fan blades, especially on axial flow fans with blades that resemble cantilever beams.

Wolf *et al.*[4] investigated the detection of cracks in a centrifugal scrubber fan. They used both Finite Element (FE) models and experimental measurements to identify the effects of artificially induced cracks on a scrubber fan blade. Experimental modal analysis was performed on the stationary fan, using an electromagnetic exciter attached to a blade with a stinger. Some success was attained although it is clear from this work that frequency based damage detection is difficult for complicated geometries such as shrouded centrifugal fans.

Sundaresan *et al.*[5] used a scanning laser vibrometer in conjunction with piezoceramic actuators for the detection of damage on a section of a wind turbine blade. The authors used changes in transmissibility, frequency response functions and operational deflection shapes to detect damage. All three techniques detected damage simulated by clamping a steel plate to the blade. Again the method required detailed measurements during stationary conditions, which is impractical for most industrial applications on critical equipment, that run uninterrupted for extended periods of time.

Schulz *et al.*[6] proposed the use of transfer functions using piezoceramic patches that served as both actuators and sensors for the detection of damage in composite helicopter blades. An advantage of this method was that it was not necessary to develop a model of the structure. The ratio of peaks and values of a transmissibility function was very sensitive to structural changes and could identify small levels of damage. Changes in the structural response due to global environmental effects were partially cancelled because transmissibility functions are the ratio of two response quantities.

These experiences suggest that a feasible on-line vibration based monitoring technique may be developed that can identify blade damage from measured natural frequencies determined continuously from the operational excitation that is present anyway under normal operating conditions. This is particularly so for axial flow fans with cantilever-like blades where the damage is likely to be caused by fatigue close to the blade root.

Such an identification approach was suggested for industrial structures by Kriel & Heyns,[7] who investigated the feasibility of detecting damage to piping structures in petro-chemical plants by making use of on-line vibration monitoring. They used AutoRegressive Moving Average Vector (ARMAV) methods to estimate modal parameters. The flow in the piping system was found to provide enough broad band excitation to excite the modes of interest. The method provided sufficiently accurate determination of natural frequencies to detect damage.

This work investigated the use of such an on-line vibration monitoring approach for axial fan blade damage detection. The investigation entailed a finite element sensitivity study, followed by an experimental investigation on a four-bladed experimental fan blade damage simulator, developed for this purpose. Vibration measurements are taken on the fan blades since measurements taken at the bearing do not contain enough information on the dynamics of individual blades. Further finite element studies are done to explain some discrepancies found between the finite element and experimentally determined results.

Finite element investigation of natural frequency shifts as damage indicators

The viability of using shifts in natural frequencies due to damage in a rotating axial flow fan blade as damage indicators was first investigated with the aid of finite element software. Since it is known that the number of elements used in the mesh, the aspect ratio of the elements and the element type used can substantially influence the natural frequencies, a simple cantilever beam is first modelled to identify suitable values of these parameters.

The results are compared to analytically calculated natural frequencies for a uniform cantilever beam (1 m long $\times$ 100 mm wide $\times$ 10 mm high) with a modulus of elasticity of 70 GPa. The results for the first four vertical (up and down) and horizontal modes (sideways) can be seen in Table I. Clearly, it is not possible to obtain accurate estimations of natural frequencies using first order, eight node brick elements. Even when a refined, high-density mesh is used, the natural frequencies differed from the analytically calculated frequencies by as much as 15 %. This phenomenon is caused by the inherent stiffness of a first order element. These elements use a constant strain integration scheme through the element, causing the element to perform poorly in bending. Since most mode shapes involve bending in the vertical or horizontal plane, this influenced the calculation of natural frequencies significantly.

The second order twenty node brick elements with midside nodes gave much improved results. These elements assume a linear distribution of strain throughout the element. This allowed for an accurate representation of the strain fields in elastic analysis. Consequently this element gave almost exact predictions of natural frequencies. Accurate results were obtained even with a very coarse mesh and poor aspect ratios for the second order elements.

After guidelines for the accurate modelling of blade-like structures had been established, a model of one blade of an experimental fan blade damage simulator (see Fig. 1) was constructed. An important difference between the stationary beam, analysed when guidelines for mesh refinement were established, and a fan blade is the centrifugal accel-

TABLE I
COMPARISON OF NATURAL FREQUENCIES FOUND FOR 1 M ALUMINIUM HINGED BEAM

Vertical natural frequencies (Hz)				
Description	Mode 1	Mode 2	Mode 3	Mode 4
Analytical values	8.23	52.40	144.34	283.06
8-node, coarse mesh (760 elements)	13.73	96.86	279.71	551.13
8-node, very fine mesh (4400 elements)	11.32	74.61	211.18	414.78
8-node, good aspect ratio (2000 elements)	8.98	56.21	157.38	308.14
20-node, coarse mesh (760 elements)	8.23	51.81	144.34	284.64
Horizontal natural frequencies (Hz)				
Description	Mode 1	Mode 2	Mode 3	Mode 4
Analytical values	74.11	471.61	1299.05	2547.56
8-node, coarse mesh (760 elements)	70.38	425.14	1127.40	2277.00
8-node, very fine mesh (4400 elements)	70.26	424.85	1128.00	2300.00
8-node, good aspect ratio (2000 elements)	74.02	447.15	1189.00	2370.00
20-node, coarse mesh (760 elements)	74.07	447.46	1189.70	2400.00

eration imposed on the blade. Fortunately, modern FE method software allows these boundary conditions to be added with relative ease. Most software packages use a stiffness matrix-updating scheme to simulate the stiffening of the structure under this load.

Fig. 1 shows the FE model for one of the simulator blades, whilst the first five natural frequencies compared with experimentally determined frequencies can be seen in Table II. Clearly, good correlation was found to exist between the FE model and the measured frequencies on the undamaged simulator blade.

TABLE II
FE MODEL RESULTS COMPARED TO EXPERIMENTAL RESULTS

Mode number	FEM value [Hz]	Experimental value [Hz]
1	34.53	33.41
2	202.40	203.31
3	285.18	285.51
4	435.13	447.32
5	562.77	563.50

The MSC MARC software used for the FE work can model the very complicated behaviour of fatigue cracking. Because these sophisticated cracking algorithms require stress factors (which can differ from measurement to measurement, even under near perfect experimental conditions) and other material properties that have to be measured experimentally, it was however decided to restrict crack modelling to simple methods that did not require any known special material properties. Damage can be simulated by untying nodes to represent a certain level of damage or decreasing the modulus of elasticity of neighbouring elements. If a very fine mesh is used, elements can also be removed (this was not practical in the present study). Untying nodes and reducing the modulus of elasticity gave similar results. Local damage, as induced on the simulator, was better simulated by untying the nodes. The percentage shift in natural frequency with damage levels of 10%, 20%, 30% and 40% (more nodes untied) can be seen in Fig. 2. It is obvious that some mode shapes are far more sensitive to damage at the root of the blade than others. Only the mode shapes that show sensitivity to damage close to the root of the blade is shown. These results seemed to indicate that natural frequency shifts will work very well as a damage level indicator.

Experimental test setup

The blade damage simulator is depicted in Fig. 3. Two piezoelectric strain gauges and one miniature piezoelectric accelerometer were used to measure the dynamic behaviour of the blade with increasing levels of damage. Damage was simulated by using a fine hacksaw to cut into the root of the blade. An additional accelerometer was attached to another blade to test the ability of the damage detection method to identify damage levels on individual blades. The FE model provided valuable insight into the placement of sensors at a position where the modes shapes, most sensitive to damage, cause maximum strain or acceleration, depending on which sensor is used. During preliminary measurements the fourth (first torsional) natural frequency was found to be very well defined. Although the predicted sensitivity of this natural frequency was not as high as the third natural frequency, special care was taken to place sensors to measure this frequency as well.

An AutoRegressive Moving Average with eXogenous signal (ARMAX) model, as described in Pandit *et al.*[8] was used to obtain a curve fit through the Power Spectral Density plots.

If $y(t)$ and $u(t)$ are scalar signals, the model structure is:

$$A\left(q^{-1}\right) y(t) = B\left(q^{-1}\right) u(t) + C\left(q^{-1}\right) e(t) \tag{1}$$

where

$$\begin{aligned} A\left(q^{-1}\right) &= 1 + a_1 q^{-1} + \ldots + a_{na} q^{-na} \\ B\left(q^{-1}\right) &= 1 + b_1 q^{-1} + \ldots + b_{nb} q^{-nb} \\ C\left(q^{-1}\right) &= 1 + c_1 q^{-1} + \ldots + c_{nc} q^{-nc} \end{aligned} \tag{2}$$

The parameter vector is taken as

$$\theta = (a_1 \ \ldots \ a_{na} \ \ b_1 \ \ldots \ b_{nb} \ \ c_1 \ \ldots \ c_{nc})^T \tag{3}$$

The model (1) can be written explicitly as a difference equation

$$\begin{aligned} y(t) &= a_1 y(t-1) + \ldots + a_{na} y(t-na) \\ &= b_1 u(t-1) + \ldots + b_{nb} u(t-nb) \\ &+ e(t) + c_1 e(t-1) + \ldots + c_{nc} e(t-nc) \end{aligned} \tag{4}$$

This model can easily be rewritten in state space format, since from (1)

$$y(t) = \frac{B\left(q^{-1}\right)}{A\left(q^{-1}\right)} u(t) + \frac{C\left(q^{-1}\right)}{A\left(q^{-1}\right)} e(t) \tag{5}$$

For this structure (5),

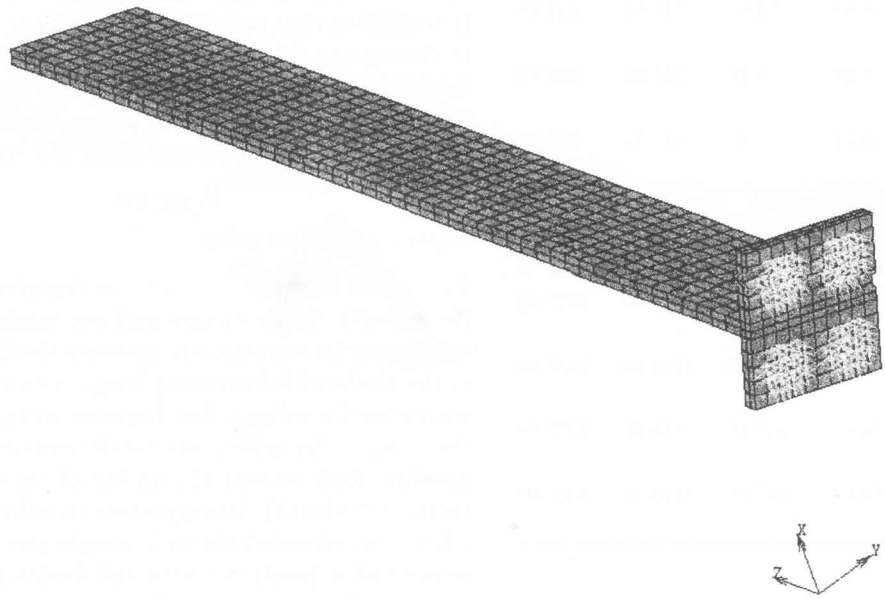

Fig. 1. FE model of the simulator blades

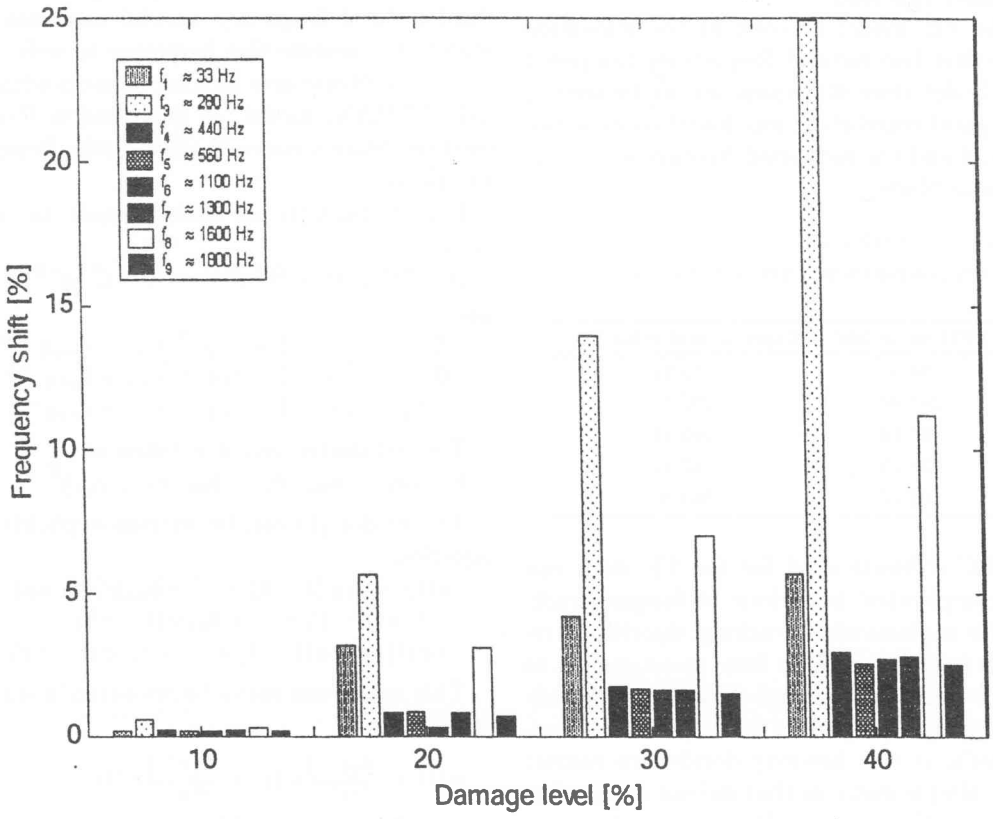

Fig. 2. Frequency shifts with increasing levels of damage

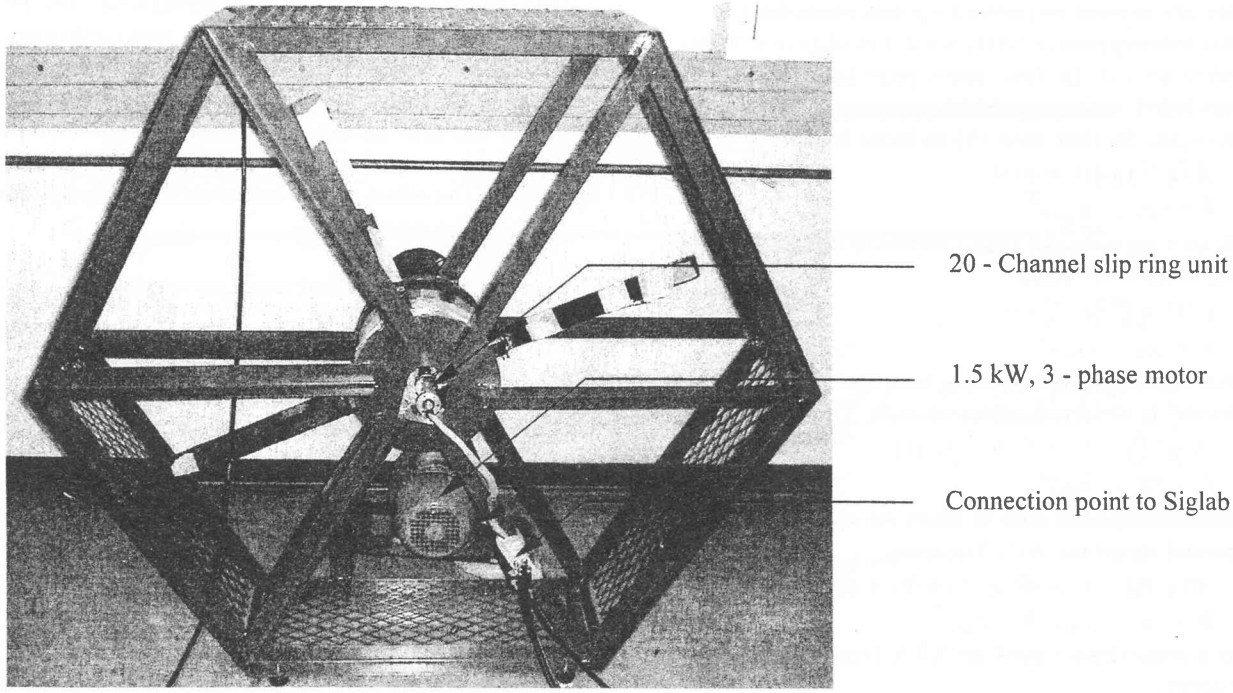

Fig. 3. Experimental fan blade damage simulator

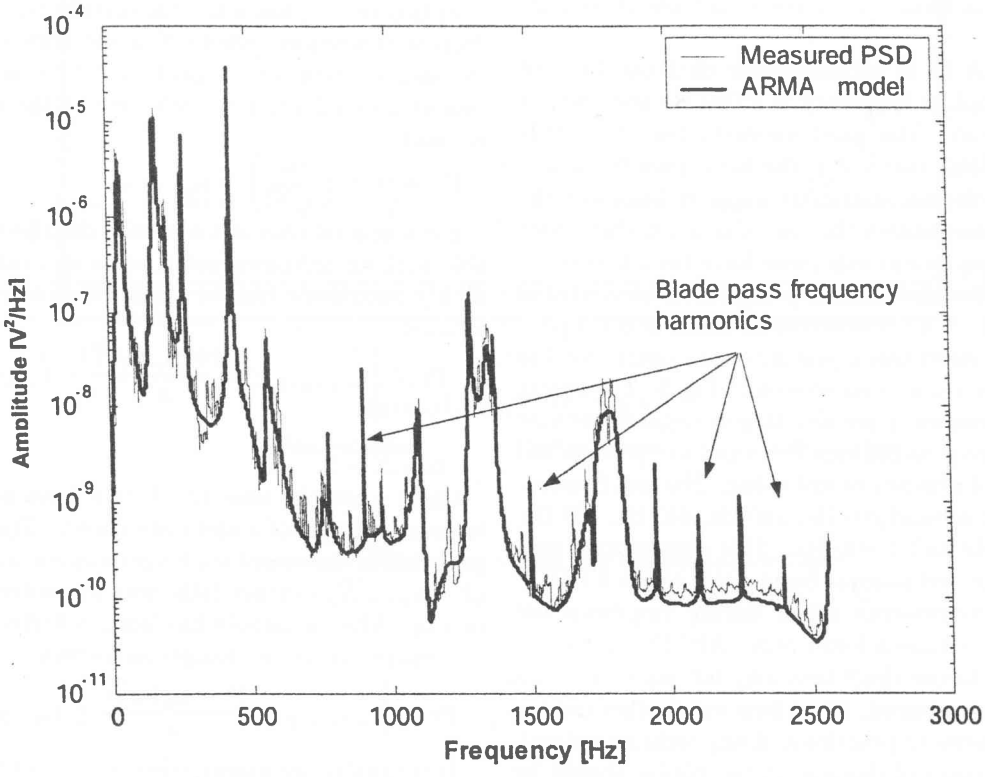

Fig. 4. Typical ARMA curve fit to accelerometer data

$$G\left(q^{-1};\theta\right) = \frac{B\left(q^{-1}\right)}{A\left(q^{-1}\right)}$$
$$H\left(q^{-1};\theta\right) = \frac{C\left(q^{-1}\right)}{A\left(q^{-1}\right)} \quad (6)$$

This format makes it possible to use the model in MATLAB.

There are several important special cases for (1)

- An autoregressive (AR) model is obtained when $nb = nc = 0$. In this case a pure time series is modelled, no input signal is assumed to be present. In that case (1) reduces to
$$A\left(q^{-1}\right) y\left(t\right) = e\left(t\right)$$
$$\theta = \left(a_1 \ \ldots \ a_{na}\right)^T \quad (7)$$
- A moving average (MA) model is obtained when $na = nb = 0$. Then
$$y\left(t\right) = C\left(q^{-1}\right) e\left(t\right)$$
$$\theta = \left(c_1 \ \ldots \ c_{nc}\right)^T \quad (8)$$
- An autoregressive moving average (ARMA) model is obtained when $nb = 0$. Then
$$A\left(q^{-1}\right) y\left(t\right) = C\left(q^{-1}\right) e\left(t\right)$$
$$\theta = \left(b_1 \ \ldots \ b_{nb}\right)^T \quad (9)$$
- Another special case is when $nc = 0$. The model structure then becomes
$$A\left(q^{-1}\right) y\left(t\right) = B\left(q^{-1}\right) u\left(t\right) + e\left(t\right)$$
$$\theta = \left(a_1 \ \ldots \ a_{na} \ \ b_1 \ldots b_{nb}\right)^T \quad (10)$$

This is sometimes called an ARX (controlled autoregressive) model.

The AR and ARMAX (reduced to an ARMA model because of the output only data) subroutines were the only models that could be used in the system identification toolbox of MATLAB. The AR model was substantially less expensive computationally but the ARMA model outperformed the latter in terms of accuracy and was chosen instead.

A typical ARMA fit to accelerometer data can be seen in Fig. 4. The sampling frequency is 2 000 Hz and the fan rotates at 750 r.p.m. The most apparent feature of this PSD and the resulting curve fit is the blade pass frequency harmonics due to the six stationary support beams of the simulator. This necessitates the use of much higher order ARMA models than would otherwise have been necessary. The speed controller also causes a high level of electrical noise to be present. A 4 s measurement taken at 600 r.p.m. and a 4 s measurement taken just after the controller has been tripped at 750 r.p.m. can be seen in Fig. 5. The effects of the blade pass frequency are also largely negated because the rotational speed changed rapidly from 750 r.p.m. to 450 r.p.m. during the 4 s measurement taken. Natural frequencies can be seen at around 200 Hz, 280 Hz, 440 Hz, 560 Hz, 1 100 Hz, 1 340 Hz and 1 800 Hz. This corresponds very well with the predicted natural frequencies of the FEM.

Whilst the measurements taken during run-down are much cleaner and require a lower order ARMA model, applications such as forced draft fans may not allow this, unless maintenance is required. Most fans will further display blade pass frequencies in practice and any technique developed for the detection of damage in fan blades should be able to cope with these effects.

Another variable of the simulator is the variable pitch blades. Fig. 6 shows measurements taken at 0°, 27° and 45° pitch angles. A certain amount of pitch is necessary to ensure enough broad band excitation for natural frequencies to be excited properly. While the second and fourth natural frequencies are not very sensitive to the pitch angle, the third is very sensitive. This was confirmed by the FE model. All subsequent measurements were taken at a pitch angle of 18°. The time signals were filtered above 25 Hz since the first natural frequency is found at 33 Hz and the first rotational frequency is 12.5 Hz (750 r.p.m.). This minimised the effect of any unbalance or misalignment still present in the simulator.

Determination of measurement parameters

It is very difficult to compute beforehand the period of time domain data that will be required for an accurate ARMA model. Since the shifts in natural frequencies due to increased damage are very small, it is important that natural frequencies of the structure can be identified with an even smaller band of uncertainty. Since long-time signals combined with a high order ARMA model result in high computational times, it is important to minimise the number of measurements and the measurement period.

An approach that can be used to determine the required number of measurements and measurement period length, is confidence intervals.[9] If a variable $x(k)$ is normally distributed (it will be in this case) with an average value of μ_x and an unknown variance (s) , the sampling distribution for the mean sample $\bar{x}$ is as follows:

$$\frac{\bar{x} - \mu_x\sqrt{N}}{s} = t_n \quad n = N - 1 \quad (11)$$

In this case t_n has a normal distribution with $n = N - 1$ degrees of freedom, where N is the number of elements in the sample data set. A probability (α) statement for the sample mean $\bar{x}$ prior to collection of the sample can then be made:

$$\mathrm{Pr}\,ob\left[\bar{x} > \left(\frac{st_n}{\sqrt{N}}\right) + \mu_x\right] = \alpha \quad (12)$$

For a general case of a normally distributed random variable with an unknown mean value and variance, the probability statement can be obtained from equation (11) as follows:

$$\mathrm{Pr}\,ob\left[t_{n;1-\alpha/2} < \frac{\left(\bar{x} - \mu_x\right)\sqrt{N}}{s} \leq t_{n;\alpha/2}\right] = 1 - \alpha \quad (13)$$

$$n = N - 1$$

Once a certain amount of data have already been collected, estimates of $\bar{x}$ and s are known. Therefore the above probability statement no longer applies, since the quantity $\left(\bar{x} - \mu_x\right)\sqrt{N}/s$ either falls into the noted limits (0 or 1) or not. After a sample has been collected the probability statement therefore changes as follows:

$$\mathrm{Pr}\,ob\left[t_{n;1-\alpha/2} < \frac{\left(\bar{x} - \mu_x\right)\sqrt{N}}{s} \leq t_{n;\alpha/2}\right] = \left\{\begin{matrix}0\\1\end{matrix}\right\} \quad (14)$$

It is usually not known whether the correct probability is

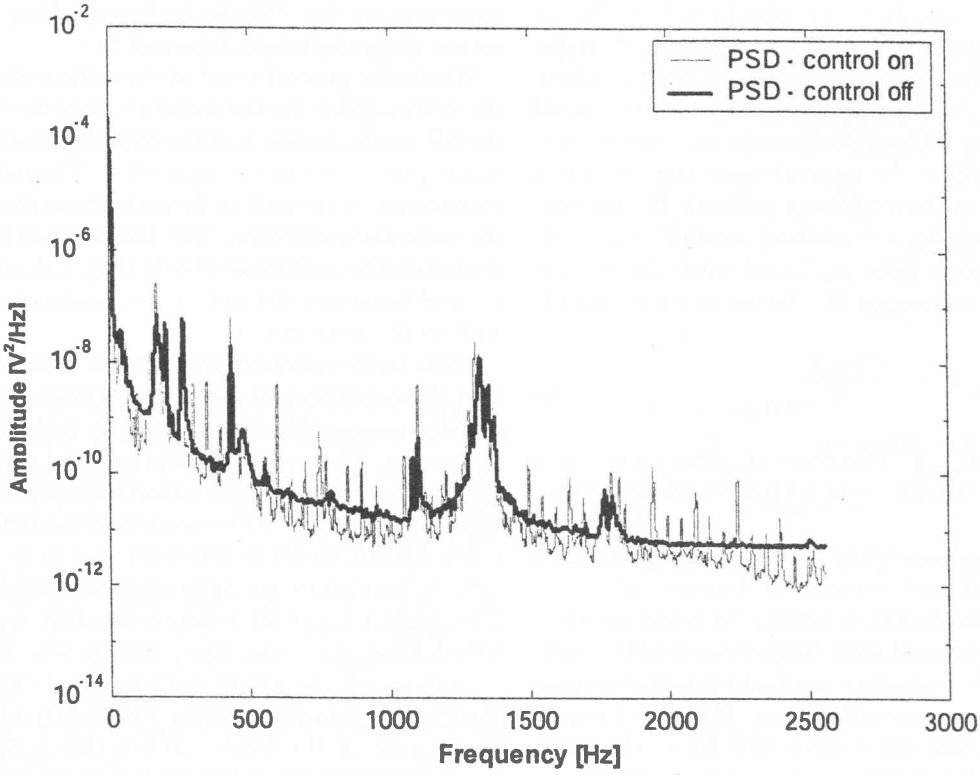

Fig. 5. Electrical noise due to speed controller on three-phase motor

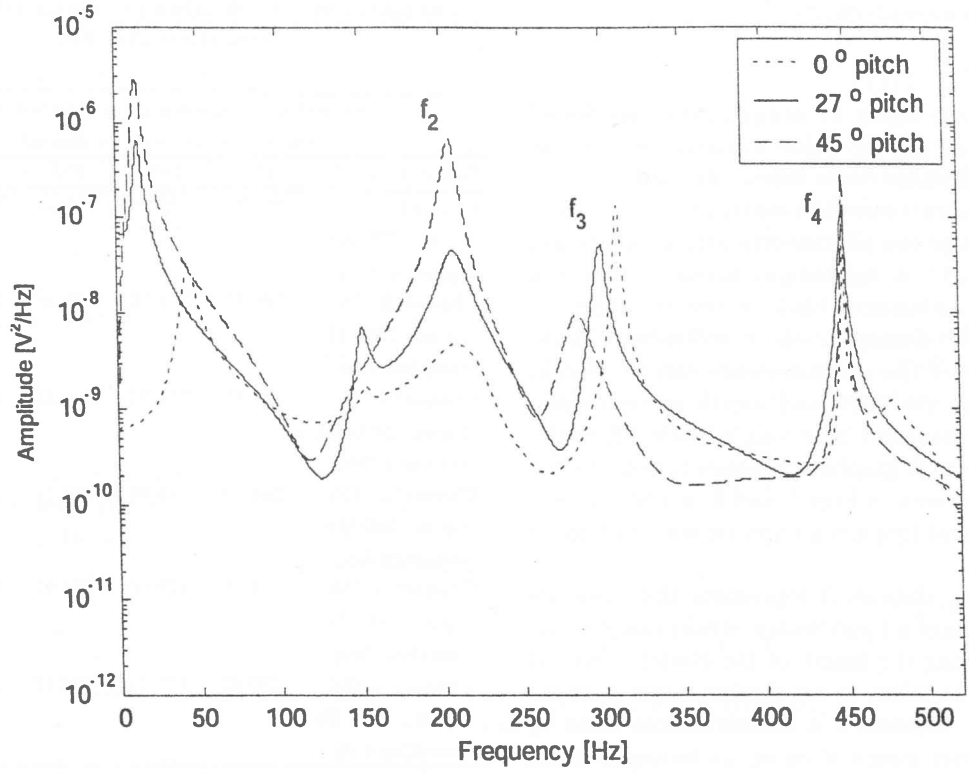

Fig. 6. The effect of different pitch angles to ARMA curve fits

zero or unity. As the value of α becomes small (the interval between $t_{n;1-\alpha/2}$ and $t_{n;\alpha/2}$ becomes larger) the probability is more likely to be unity than zero. If a large number of sample sets are collected and $\bar{x}$ and s computed for each sample, the value in equation (13) should fall within the noted interval for about $1-\alpha$ of the samples. A statement can therefore be made concerning the interval where the quantity $(\bar{x}-\mu_x)\sqrt{N}/s$ would be found with a small degree of uncertainty. These statements are called confidence statements, whilst the interval associated with this statement is known as the confidence interval. For the case of a mean value estimate, a confidence interval can be established for the mean value μ_x based upon the sample values $\bar{x}$ and s by rearranging the terms in equation (13) as follows:

$$\bar{x}-\frac{st_{n;\alpha/2}}{\sqrt{N}} \le \mu_x < \bar{x}+\frac{st_{n;\alpha/2}}{\sqrt{N}} \qquad (15)$$
$$n = N-1$$

because $t_{n;1-\alpha/2} = t_{n;\alpha/2}$. Therefore, the true mean value μ_x falls within the stated interval with a confidence of $(1-\alpha)100$ percent.

The frequencies corresponding with the third and fourth mode shapes showed most promise as damage indicators. By using different lengths and numbers of measurements, it was found that the values of these frequencies could be measured within a 99.5% confidence interval while still keeping computer time within reasonable limits. If twelve 4-s measurements are used, the mean value will fall in the range of $279.88 \le \mu_x < 280.44$ for the third natural frequency and $446.95 \le \mu_x < 447.20$ for the fourth natural frequency. This translates into a maximum error of 0.32% for the third and 0.06% for the fourth natural frequency, due to measurement errors. All subsequent experimental results are the average of twelve 4-s measurements.

Experimental results

Measurement sets were taken at sampling frequencies of 500 Hz, 1 000 Hz, and 2 000 Hz. After initial measurements with no structural damage were taken, damage of 10%, 20%, 30%, and 40% were induced by cutting into the root of a blade instrumented by two piezoelectric strain gauges and a micro accelerometer. A lightweight accelerometer was also mounted on an undamaged blade to test the ability of the technique to detect damage levels on individual blades.

Examples of some of the measurements can be seen in Tables III and IV for the third and fourth mode shapes. Frequency shifts as predicted by a single blade FE model can be seen in Table V. A graphical representation of some measurements can be seen in Figs. 7 and 8, whilst the percentage shift in natural frequencies can be seen in Figs. 9 and 10, respectively.

For all the figures, channel 3 represents the measurements taken by means of a piezoelectric strain gauge at the root of the blade (along the length of the blade). Channel 2 is the measurements taken by an accelerometer near the tip of the fan blade. Channel 1 is measurements taken by a second accelerometer mounted on an undamaged blade, whilst channel 4 is strain gauge measurements on the same blade as channel 3, but along the width of the blade. In Figs. 7–10, only channel 1 is not shown because no damage was induced on the blade measured by channel 1. Measurements over the width of the blade (channel 4) showed this measurement direction to be less sensitive than measurements along the length (channel 3).

Whilst the general trend of the shifts with increasing levels of damage for the third natural frequency is the same for the FE model results and the experimental results, the FE model predicted a much larger shift. The natural frequency corresponding to the fourth mode shape showed much better correlation however. The third natural frequency also shifted on the undamaged blade (Fig. 11), whilst the fourth natural frequency did not. This phenomenon will be dealt with in the next section.

From these examples of measured data, it was apparent that the experimental fan blade damage simulator experienced a measurable frequency shift with increasing levels of damage. The measurements sampled at 500 Hz tend to give more consistent results than measurements sampled at higher frequencies. This could be expected since a higher order ARMA model is necessary and more blade pass frequency harmonics are present in the resulting spectrum. The ARMA curve fit is more accurate when only a few well-defined peaks and valleys are present in the PSDs.

Because of the stress distribution found in most fan blades, the maximum stress will nearly always be found at the root of the blade. When this is the case, results from the experimental fan blade damage simulator showed that damage could be detected accurately using output only data and frequency shifts.

TABLE III
FREQUENCY SHIFTS FOR VARIOUS CHANNELS AND OPERATING CONDITIONS (280 Hz)

	3rd natural frequency (Hz) variation with increasing amounts of damage				
Description	0%	10%	20%	30%	40%
Channel 1, 450 r.p.m., 500 Hz sampling freq.	284.72	279.96	275.64	271.38	266.50
Channel 2, 750 r.p.m., 1000 Hz sampling freq.	280.13	274.10	268.38	268.00	262.97
Channel 2, 750 r.p.m., 2000 Hz sampling freq.	278.87	277.93	268.42	267.81	262.89
Channel 3, 450 r.p.m., 500 Hz sampling freq.	284.72	279.96	274.57	270.68	266.50
Channel 3, 750 r.p.m., 500 Hz sampling freq.	279.96	279.60	274.92	270.68	266.50
Channel 3, 450 r.p.m., 1000 Hz sampling freq.	280.92	279.74	274.67	270.46	266.31

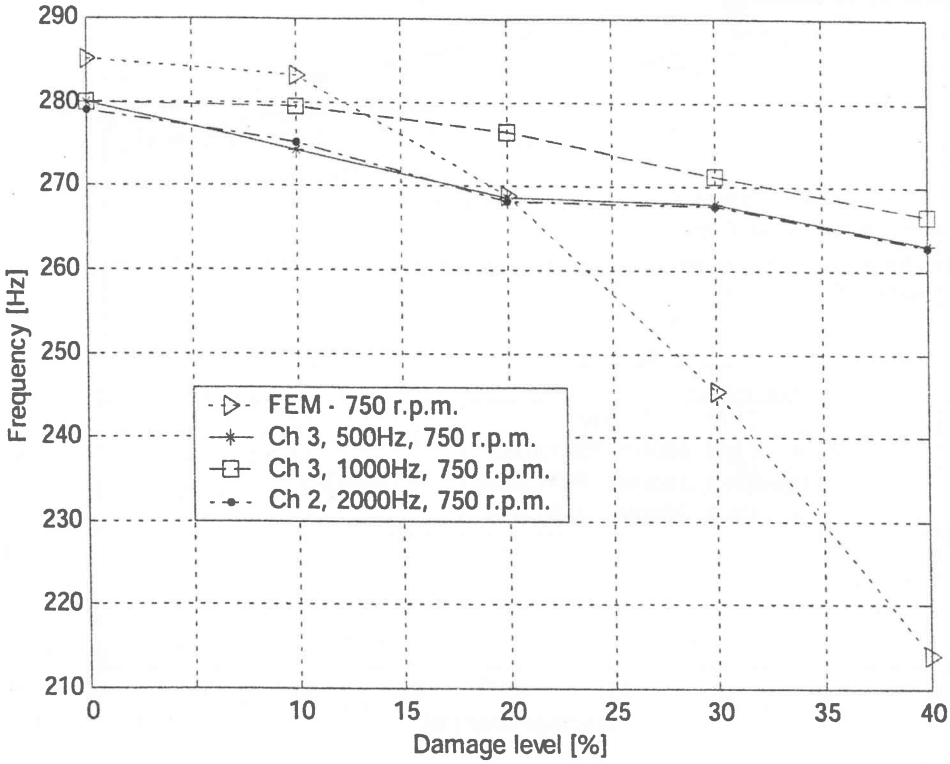

Fig. 7. The shift in the 3rd natural frequency with increasing levels of damage

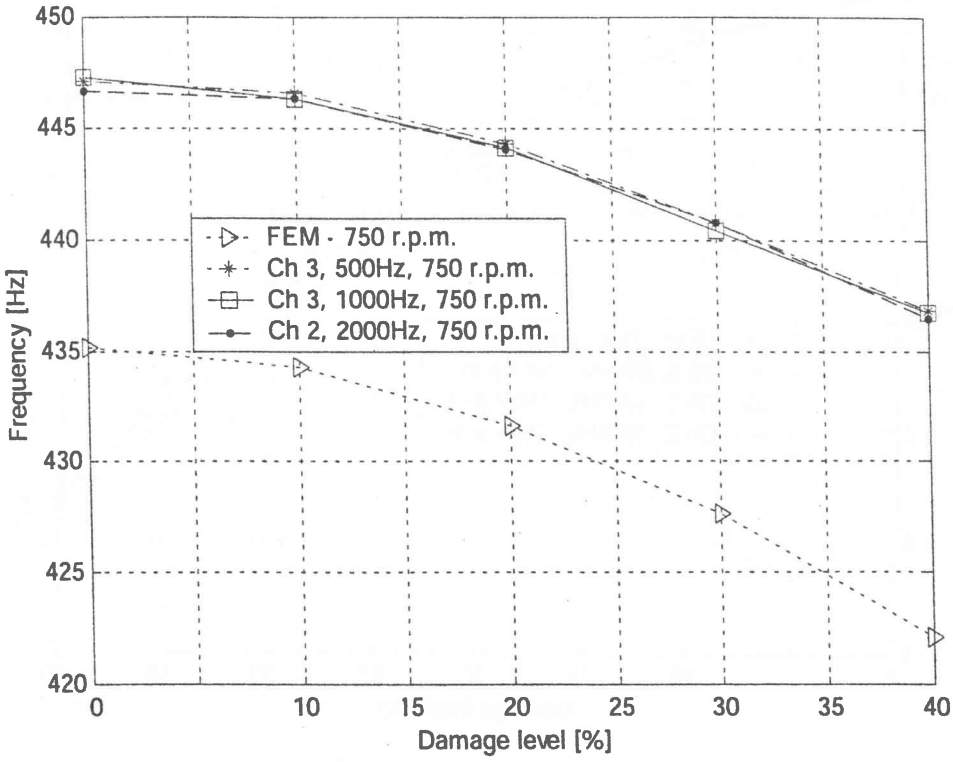

Fig. 8. The shift in the 4th natural frequency with increasing levels of damage

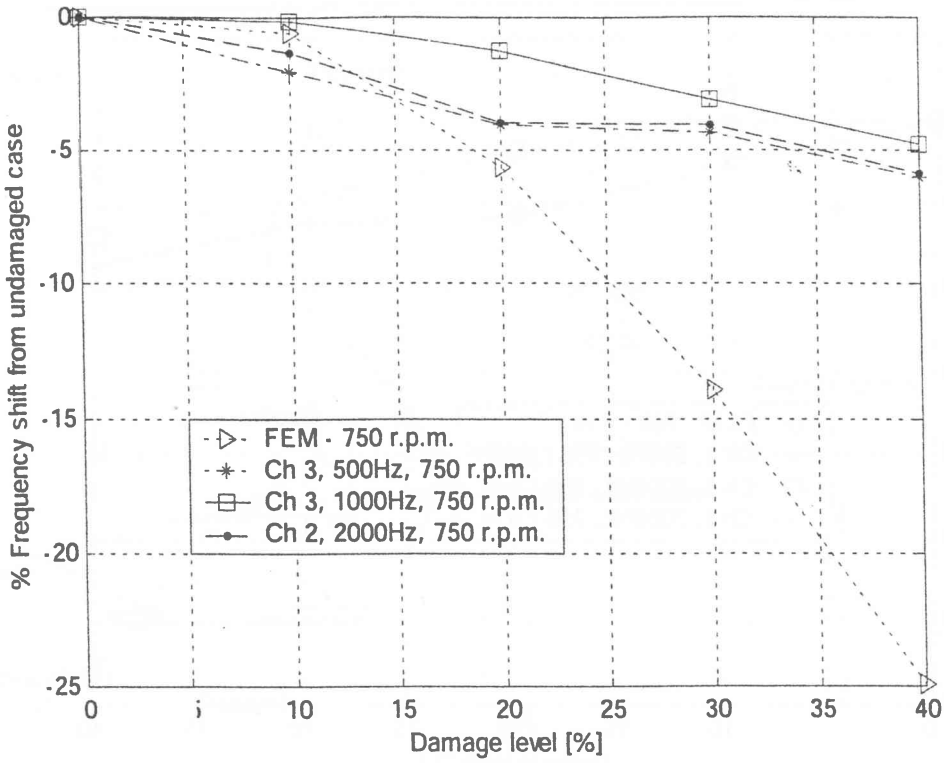

Fig. 9. Percentage shift in natural frequency for the 3rd mode shape

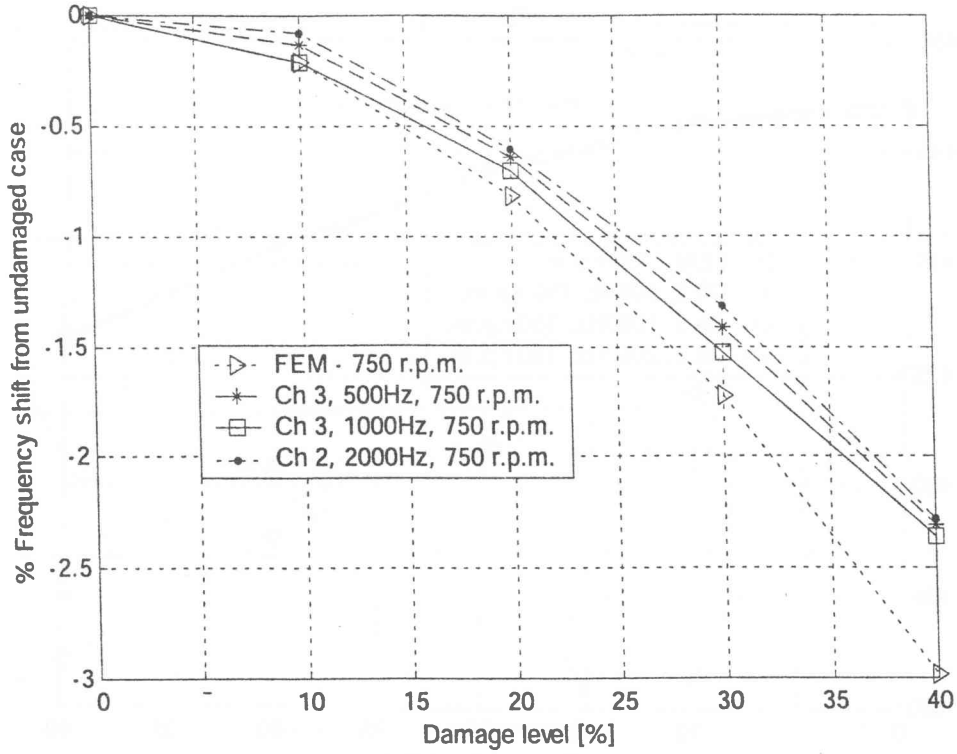

Fig. 10. The percentage shift of the 4th natural frequency

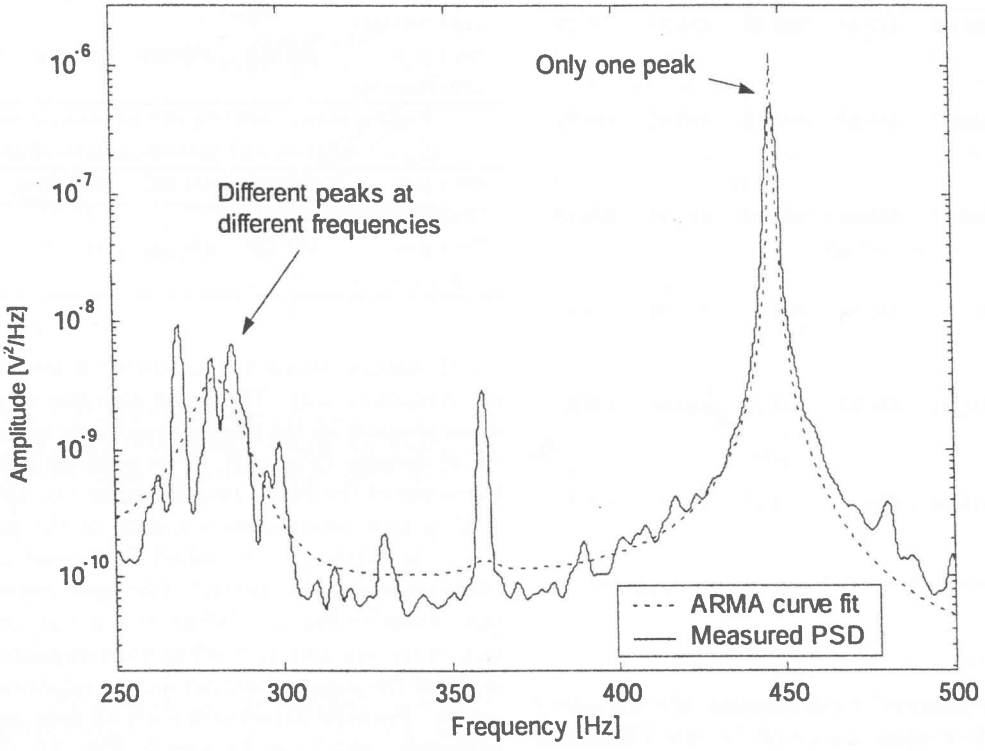

Fig. 11. Global behaviour of the test structure

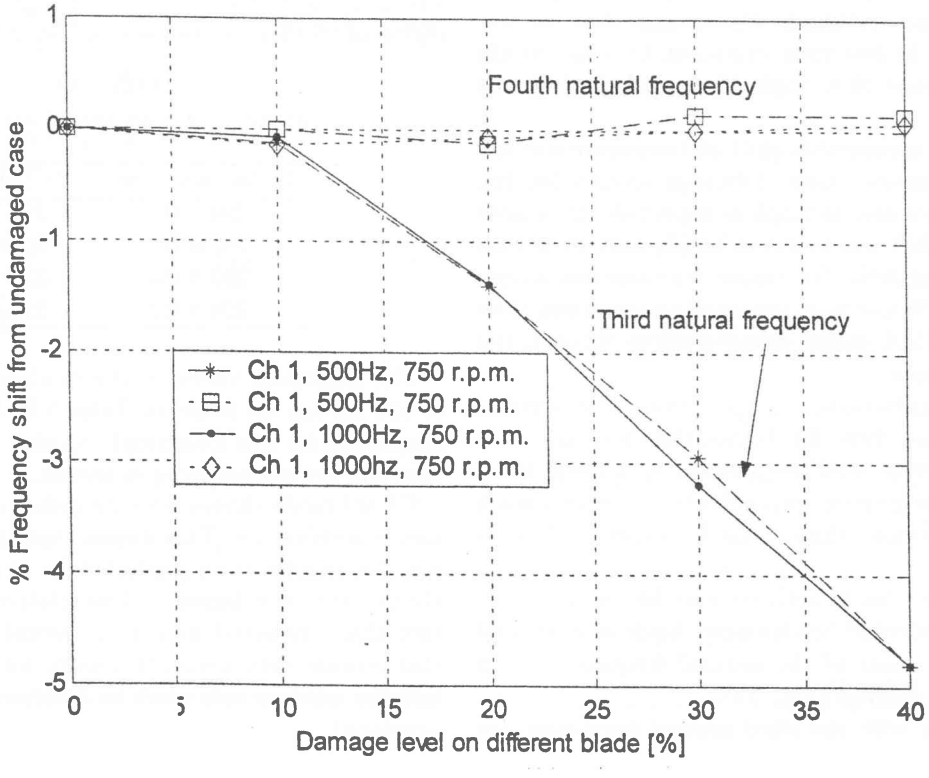

Fig. 12. Measurements taken on the undamaged blade

TABLE IV
FREQUENCY SHIFTS FOR VARIOUS CHANNELS AND OPERATING CONDITIONS (430 Hz)

4th natural frequency (Hz) variation with increasing amounts of damage					
Description	0%	10%	20%	30%	40%
Channel 1, 450 r.p.m., 500 Hz sampling freq.	435.68	435.68	435.68	436.25	435.25
Channel 2, 750 r.p.m., 1000 Hz sampling freq.	446.97	446.34	444.15	440.42	436.72
Channel 2, 750 r.p.m., 2000 Hz sampling freq.	446.67	446.16	444.14	440.46	436.48
Channel 3, 450 r.p.m., 500 Hz sampling freq.	446.55	446.55	444.24	440.80	436.81
Channel 3, 750 r.p.m., 500 Hz sampling freq.	446.55	446.55	444.24	440.80	436.81
Channel 3, 450 r.p.m., 1000 Hz sampling freq.	447.28	446.34	444.15	440.42	440.42

Global and local modes

Owing to the discrepancies found between the frequency shifts of some mode shapes predicted by the FE model and the actual measured shifts, further investigation was deemed necessary. It was postulated that the most likely cause for this phenomenon is that the measured frequencies corresponded to global frequencies of the entire structure, and that the tacit assumption of a blade acting like a single cantilever beam is not justified. This means that the frequency shift might be less than predicted by what would be a local mode shape of a single blade modelled by the FE model.

Whilst a readily measurable shift of frequency was experienced with increasing levels of damage around 280 Hz, the shift was nowhere near as much as expected. At around 40 % damage, the shift was found to be 6% compared with the predicted shift of 25%. The reason for these results can be seen in Fig. 11. While four discernible peaks exist close to 280 Hz, the ARMA model fitted a curve through the average of these peaks.

The reason for this behaviour is that. this mode is global in nature. The other three fan blades therefore also take part at slightly different local frequencies. As a result these local modes are superimposed on each other to give a much more complex behaviour than could be expected from a single blade.

Further proof for this hypothesis can be found in the fact that an instrumented, undamaged blade also showed frequency shifts at most of the natural frequencies with increasing levels of damage (Fig. 12).

In sharp contrast with the third natural frequency, the fourth natural frequency produced a well-defined peak at one frequency only. This peak also stayed at virtually the same position on the undamaged blade with increasing levels of damage (Fig. 12). The peak at 360 Hz is the 7th harmonic of the blade pass frequency at 450 r.p.m.

TABLE V
FREQUENCY SHIFTS PREDICTED BY THE SINGLE BLADE FE MODEL

Finite element model for the 3rd natural frequency (Hz) variation with increasing levels of damage					
Description	0%	10%	20%	30%	40%
450 r.p.m. 1240 elements	248.850	283.097	268.863	245.229	213.756
750 r.p.m. 1240 elements	285.018	283.266	268.978	245.352	213.992
Finite element model for the 4th natural frequency (Hz) variation with increasing levels of damage					
450 r.p.m. 1240 elements	434.932	434.023	431.429	427.463	421.905
750 r.p.m. 1240 elements	435.132	434.226	431.588	427.624	422.146

To gain a better understanding of the behaviour of the complete system, a simplified FE model of the hub and blade interface was created. The finite element model used can be seen in Fig. 13. Whilst it is not an exact representation of the simulator, it adequately explained the different shifts of frequency observed during experimental measurements. Periodic structures such as fans exhibit mode localisation, which can be seen in Fig. 14. Only one of the fan blades takes part in the first mode shape. Even when no fan blades were damaged, the mode shapes and corresponding natural frequencies differed significantly from each other. It explains the four peaks observed in Fig. 11. The numerical values of the different mode shapes in the region of 280 Hz can be seen in Table VI.

TABLE VI
COMPARISON OF MODE SHAPES AROUND 280 Hz

Undamaged case	25% damage
294.1 Hz	293.7 Hz
282.0 Hz	267.4 Hz
292.8 Hz	286.7 Hz
294.8 Hz	294.8 Hz

The numerical values of the mode shapes in the region of 433 Hz can be found in Table VII. Clearly, these mode shapes are far less influenced by other blades in the structure and are almost local in nature.

Global mode shapes provide global damage level indicators of a structure. This means that the shift in frequency may be smaller than predicted by a local model, due to the fact that the damage is less relative to the whole structure than predicted by a local model. Local models can still provide very accurate results for most mode shapes and the answers only start to deteriorate when damage is simulated.

TABLE VII
COMPARISON OF MODE SHAPES AROUND 433 Hz

Undamaged case	25% damage
433.4 Hz	429.3 Hz
433.6 Hz	433.5 Hz
433.8 Hz	433.6 Hz
434.0 Hz	433.9 Hz

CONCLUSIONS

This paper presents an approach to on-line damage detection in fan blades based on the measurement of frequency shifts. Damage usually occurs very close to the root of a blade due to the stress distribution found in a rotating structure unless some external influence, such as a contaminated working fluid, is present. An FE model shows that certain mode shapes are more sensitive to damage at the root of a blade than others. Measurements taken at bearings or on other parts of a fan structure do not contain enough information about the dynamic behaviour of the blades. Sensors mounted directly on the blade, with the exact location carefully chosen to maximise the sensitivity to chosen mode shapes, do provide detailed information on the damage level of the blade.

Due to rapid progress in computer technology and software, it is now possible to use powerful FE packages on desktop systems. This makes it possible to study the effect of damage on the dynamics of a structure such as a blade prior to construction of a test structure. Element choice and mesh refinement are extremely important. Second order elements must be used whenever possible. Although it is easy to simplify symmetric structures such as fans, careful consideration has to be given to global dynamics. Some mode shapes are local and are very valuable when individual blades have to be monitored, but most mode shapes are global.

By making use of sensors on the blades themselves, it is possible to do on-line health monitoring of critical industrial equipment such as fan blades. Even relatively small damage levels can be detected using one sensor per blade without interruption of operation.

REFERENCES

[1] Doebling SW, Farrar CR, Prime MB & Shevitz DW. Damage identification and health monitoring of structural and mechanical systems from changes in their vibration characteristics: a literature review. *Los Alamos National Laboratory Report, LA-13070-MS*, 1996.

[2] Friswell MI & Penny JET. Is damage location using vibration measurements practical? *EUROMECH 365 International Workshop: DAMAS 97, Structural Damage Assessment using Advanced Signal Processing Procedures*. Sheffield, UK, 1997.

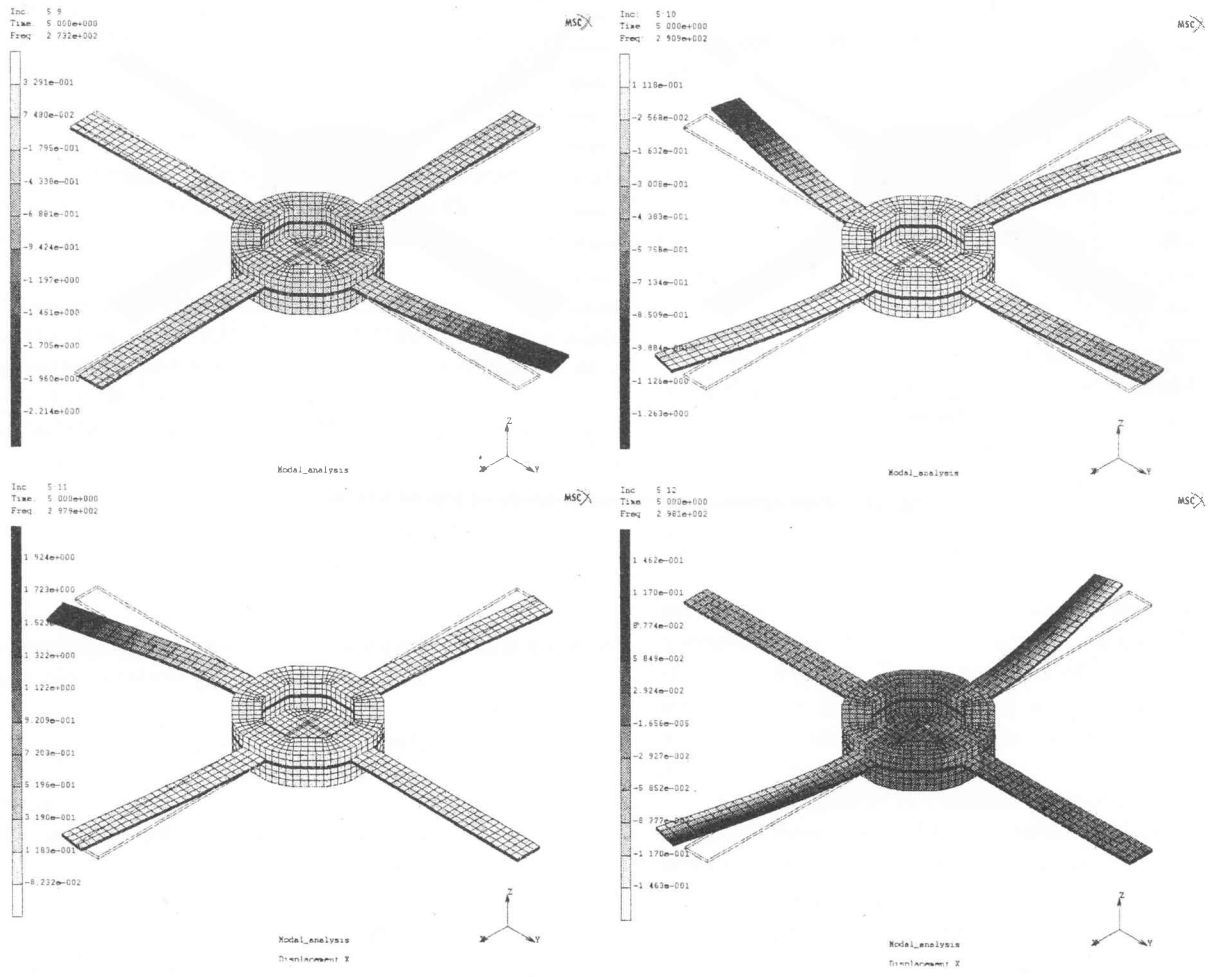

Fig. 13. Global dynamics of the damage simulator around 280 Hz

[3] e Silva JMM & de Araujo Gomes AJM.Crack Identification of simple structural elements through the use of natural frequency variations: the inverse problem. *Proceedings of the 12th International Modal Analysis Conference*, **2**, pp.1728–1735, 1994.

[4] Wolff PJ & Patrick AM. Experimental and finite element investigation of blade cracking in a scrubber fan model. *Proceedings of the 7th International Modal Analysis Conference*, **1**, pp.119–123, 1989.

[5] Sundaresan MJ, Schulz MJ, Hill J, Wheater EA, Ferguson F & Pai PF. Damage Detection on a Wind Turbine Blade Section. *Proceedings of the 17th International Modal Analysis Conference*, pp.1359–1365, 1999.

[6] Schulz MJ, Naser AS, Pai PF & Chung J. Locating Structural Damage Using Frequency Response Reference Functions. *International Workshop on Structural Health Monitoring*, Stanford University, Stanford, CA.

[7] Kriel CJ & Heyns PS. Damage identification on piping systems using on-line monitoring of dynamic properties. *Proceedings of the 16th International Modal Analysis Conference*, pp.482–488, 1998.

[8] Pandit SM. *Modal and spectrum analysis: data dependent systems in state space*. John Wiley & Sons, 1991.

[9] Bendat JS & Piersol AG. *Measurement and analysis of random data*. John Wiley & Sons, 1967.

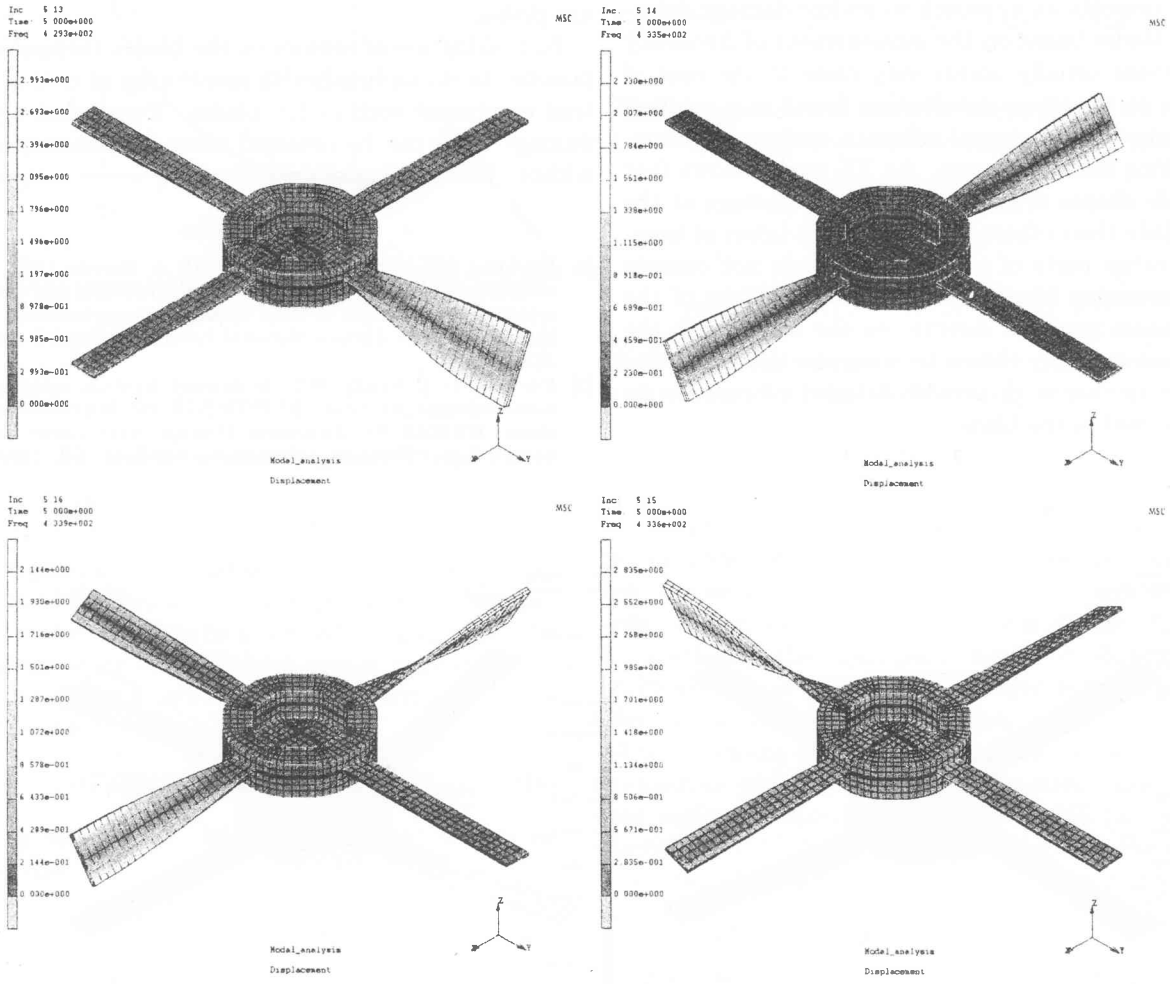

Fig. 14. Global dynamics of the damage simulator around 433 Hz